

# Hole spin relaxation in $p$ -type (111) GaAs quantum wells

L. Wang and M. W. Wu\*

*Hefei National Laboratory for Physical Sciences at Microscale and Department of Physics,  
University of Science and Technology of China, Hefei, Anhui, 230026, China*

(Dated: November 18, 2018)

Hole spin relaxation in  $p$ -type (111) GaAs quantum wells is investigated in the case with only the lowest hole subband, which is heavy-hole like in (111) GaAs/AlAs and light-hole like in (111) GaAs/InP quantum wells, being relevant. The subband Löwdin perturbation method is applied to obtain the effective Hamiltonian including the Dresselhaus and Rashba spin-orbit couplings. Under a proper gate voltage, the total in-plane effective magnetic field in (111) GaAs/AlAs quantum wells can be strongly suppressed in the whole momentum space, while the one in (111) GaAs/InP quantum wells can be suppressed only on a special momentum circle. The hole spin relaxation due to the D'yakonov-Perel' and Elliott-Yafet mechanisms is calculated by means of the fully microscopic kinetic spin Bloch equation approach with all the relevant scatterings explicitly included. For (111) GaAs/AlAs quantum wells, extremely long heavy-hole spin relaxation time (upto hundreds of nanoseconds) is predicted. In addition, we predict a pronounced peak in the gate-voltage dependence of the heavy-hole spin relaxation time due to the D'yakonov-Perel' mechanism. This peak origins from the suppression of the unique inhomogeneous broadening in (111) GaAs/AlAs quantum wells. Moreover, the Elliott-Yafet mechanism influences the spin relaxation only around the peak area due to the small spin mixing between the heavy and light holes in quantum wells with small well width. We also show the anisotropy of the spin relaxation. In (111) GaAs/InP quantum wells, a mild peak, similar to the case for electrons in (111) GaAs quantum wells, is also predicted in the gate-voltage dependence of the light-hole spin relaxation time. The contribution of the Elliott-Yafet mechanism is always negligible in this case.

PACS numbers: 72.25.Rb, 71.70.Ej, 71.55.Eq, 73.21.Fg

## I. INTRODUCTION

Spin dynamics in semiconductor quantum wells (QWs) has been intensively investigated in recent years due to the fast development of semiconductor spintronics.<sup>1-7</sup> In III-V zinc-blende QW systems, spin relaxation is mainly determined by the D'yakonov-Perel' (DP) mechanism,<sup>8</sup> which results from the momentum scattering together with the momentum-dependent effective magnetic field induced by the Dresselhaus<sup>9</sup> and/or Rashba<sup>10</sup> spin-orbit couplings (SOCs). So far, most studies focus on the (001)<sup>11-28</sup> and (110) QWs.<sup>29-35</sup> In these works, many efforts have been devoted to obtain a long spin relaxation time (SRT).<sup>11,14,15,18-22,24-27,29,33,34</sup> In (001) QWs, when the strengths of the Dresselhaus and Rashba terms are comparable, electron spin relaxation along the [110] or  $[\bar{1}\bar{1}0]$  direction can be strongly suppressed.<sup>11,14,15,18-22,24-27</sup> For (110) symmetric QWs, the effective magnetic field due to the Dresselhaus term is oriented along the growth direction, which leads to an absent DP relaxation for electron spins along this direction.<sup>29,33,34</sup>

Recently, some attention has been devoted to (111) QWs where electron spin relaxation also shows rich properties.<sup>36-40</sup> Cartoixa *et al.*<sup>36</sup> pointed out that to the first order in the momentum, the effective magnetic field from both the Dresselhaus and Rashba terms  $\Omega_1 = (\alpha_D + \alpha_R)(k_y, -k_x, 0)$  (with  $z \parallel [111]$ ,  $x \parallel [\bar{1}1\bar{2}]$  and  $y \parallel [\bar{1}10]$ ), can be suppressed to zero by setting the Rashba coefficient  $\alpha_R$  to cancel with the Dresselhaus coefficient  $\alpha_D$

and hence the DP spin relaxation becomes absent for all three spin components. However, this strict cancellation can not occur due to the existence of the cubic Dresselhaus term  $\Omega_3 = \frac{\gamma}{2\sqrt{3}}[-k^2 k_y, k^2 k_x, \sqrt{2}(3k_x^2 k_y - k_y^3)]$ . Sun *et al.*<sup>38</sup> showed that with this cubic term included, the cancellation occurs only for the in-plane effective magnetic field on a special momentum circle, which may lead to a peak in the density or temperature dependence of the SRT. Experimentally, Balocchi *et al.*<sup>40</sup> measured the gate-voltage dependence of the SRT and a two-order of magnitude increase of the SRT can be observed, reaching values larger than 30 ns by applying an external electric field of 50 kV/cm along the growth direction of the QW. However, to the best of our knowledge, there are still no reports on hole spin relaxation in (111) zinc-blende QWs.

In the present work, we investigate the hole spin relaxation in  $p$ -type (111) GaAs QWs with only the lowest subband being relevant. In GaAs/AlAs QWs, the lowest hole subband is heavy-hole (HH) like. The Dresselhaus and Rashba SOC terms of the lowest HH subband  $\Omega_{D(R)}^h$  can be written as

$$\Omega_D^h = [\beta_x^h(3k_x^2 k_y - k_y^3), \beta_y^h(k_x^3 - 3k_x k_y^2), \beta_z^h(3k_x^2 k_y - k_y^3)], \quad (1)$$

$$\Omega_R^h = [\alpha_x^h(3k_x^2 k_y - k_y^3), \alpha_y^h(k_x^3 - 3k_x k_y^2), \alpha_z^h(3k_x^2 k_y - k_y^3)]eE_z, \quad (2)$$

respectively, which are obtained by the subband Löwdin partitioning method.<sup>41,42</sup> The coefficients are given in

Appendix A. Here,  $E_z$  is the electric field along the growth direction. It is noted that the Rashba term  $\Omega_R^h$  has not been reported in the previous literature and interestingly its component  $\Omega_{Ri}^h$  ( $i = x, y, z$ ) can be strictly cancelled by the corresponding Dresselhaus one  $\Omega_{Di}^h$  by setting the gate voltage

$$E_z^i = -\beta_i^h / (e\alpha_i^h). \quad (3)$$

The cancellation gate voltages  $E_z^x$  (about 20 kV/cm) and  $E_z^y$  (about 22 kV/cm) are close to each other, indicating that the in-plane components of the effective magnetic field can be strongly suppressed. This cancellation leads to a strong suppression of the in-plane inhomogeneous broadening<sup>43</sup> and hence an extremely long SRT for spins along the growth direction. It is further noted that although the out-of-plane component of the effective magnetic field of the lowest HH subband can also be suppressed to zero, the cancellation gate voltage  $E_z^z$  (about 10<sup>3</sup> kV/cm) is too large to realize. Therefore, a large anisotropy between the in-plane and out-of-plane spin relaxations is expected.

We also investigate the hole spin relaxation in GaAs/InP QWs where the lowest hole subband is light-hole (LH) like. The Dresselhaus and Rashba SOC terms are then given by

$$\Omega_D^l = [(\beta_x^{l1}\mathbf{k}^2 + \beta_x^{l2}\langle k_z^2 \rangle)k_y, -(\beta_x^{l1}\mathbf{k}^2 + \beta_x^{l2}\langle k_z^2 \rangle)k_x, \beta_z^l(3k_x^2k_y - k_y^3)], \quad (4)$$

$$\Omega_R^l = [\alpha_x^l\mathbf{k}^2k_y, -\alpha_x^l\mathbf{k}^2k_x, \alpha_z^l(3k_x^2k_y - k_y^3)]eE_z, \quad (5)$$

respectively. One finds that similar to the case of electrons in (111) QWs,<sup>38</sup> the in-plane components of these two terms can be suppressed to zero only on a special momentum circle. The out-of-plane component can also be suppressed to zero under an unrealistic gate voltage.

We calculate the hole spin relaxation by the kinetic spin Bloch equation (KSBE) approach,<sup>5,12</sup> with all the relevant scatterings explicitly included. As the Elliott-Yafet<sup>44</sup> (EY) mechanism is the leading spin relaxation mechanism in hole spin relaxation in bulk,<sup>45</sup> we calculate the SRT due to both the DP and EY mechanisms in the present work. For (111) GaAs/AlAs QWs, we find that the EY mechanism is negligible unless the DP mechanism can be greatly suppressed. By tuning the gate voltage, we predict a pronounced peak in the SRT where the SRT can be extremely long (upto hundreds of nanoseconds). This property is favorable for spin manipulation, storage and device design. This peak results from the suppression of the unique inhomogeneous broadening<sup>43</sup> in (111) QWs. The effects of hole density, temperature and impurity density on the suppression of the spin relaxation are investigated. We also analyze the anisotropy of the spin relaxation. For (111) GaAs/InP QWs, a peak is also predicted in the gate-voltage dependence of the SRT. However, the peak becomes less pronounced compared with the case in (111) GaAs/AlAs QWs. The contribution of the EY mechanism is demonstrated to be negligible to the predicted properties.

This paper is organized as follows. In Sec. II, the effective Hamiltonian of the lowest hole subband in (111) GaAs/AlAs and GaAs/InP QWs is derived. The KSBEs are also constructed in this section. Then in Sec. III, we investigate the hole spin relaxations in GaAs/AlAs and GaAs/InP QWs respectively. We summarize in Sec. IV.

## II. EFFECTIVE HAMILTONIAN AND KSBES

We start our investigation from the  $p$ -type (111) GaAs/AlAs and GaAs/InP QWs. The HH and LH can be described by the  $4 \times 4$  Hamiltonian

$$H_{4 \times 4} = H_L + H_{8v8v}^b + H_\epsilon + V(z)I_4 + H_E I_4, \quad (6)$$

since the contribution from the conduction and split-off bands is marginal in the present calculation. Here,  $H_L = H_L^{(0)} + H_L^{(\parallel)}$  is the Luttinger Hamiltonian<sup>46</sup> with  $H_L^{(0)}$  corresponding to the part with  $k_{x,y} = 0$ ,  $H_{8v8v}^b$  is the Dresselhaus SOC of the HH and LH bands<sup>9</sup> and  $H_\epsilon$  stands for the strain Hamiltonian based on the theory of Bir and Pikus.<sup>42,47</sup> Their expressions are given in Appendix B.  $V(z)$  is the confinement applied along the growth direction within the infinite-depth well potential approximation and  $I_4$  is a  $4 \times 4$  unit matrix.  $H_E = -eE_z z$  represents the electric field term, which is the source of the Rashba SOC.<sup>10</sup>

By solving the Schrödinger equation of  $H_0 = H_L^{(0)} + V(z)I_4 + H_\epsilon$ , the subband energies for the HH and LH are given by

$$E_{n_z}^{h,l} = \frac{n_z^2 \pi^2 \hbar^2}{2m_z^{h,l} a^2} \mp E_S^1 - E_S^2, \quad (7)$$

where  $n_z$  stands for the subband index along the growth direction,  $a$  is the well width and  $m_z^{h,l} = \frac{m_0}{\gamma_1 \mp 2\gamma_3}$  represents the effective masses of the HH and LH along the  $z$ -axis.  $\gamma_{1,3}$  and  $m_0$  stand for the Kohn-Luttinger parameters and the free electron mass, respectively. The contributions of the strain  $E_S^1$  and  $E_S^2$  are given in Eqs. (B4) and (B5) in Appendix B. It is noted that  $E_S^2$  is just an energy shift for all the HH and LH subbands and can be neglected in the present calculation. For GaAs/AlAs QWs, the contribution of the strain is neglected due to the extremely small lattice mismatch and hence the lowest hole subband is HH like. However, for GaAs/InP QWs, due to the existence of strain, the lowest hole subband is LH like. In our calculation, we focus on the case with only the lowest hole subband being relevant while other subbands have much higher energies.

We first construct the effective Hamiltonian of the lowest hole subband in (111) GaAs QWs by the subband Löwdin partitioning method<sup>41,42</sup> upto the third order of the in-plane momentum. The effective Hamiltonian of the lowest hole subband in (111) GaAs/AlAs QWs can be written as

$$H_{\text{eff}}^h = \epsilon_{\mathbf{k}}^h + (\Omega_D^h + \Omega_R^h) \cdot \frac{\boldsymbol{\sigma}}{2}. \quad (8)$$

Here,  $\varepsilon_{\mathbf{k}}^h = \frac{\hbar^2 \mathbf{k}^2}{2m_t^h}$ , with the in-plane effective mass  $m_t^h$  given in Appendix A, and  $\boldsymbol{\sigma}$  are the Pauli matrices. The Dresselhaus and Rashba SOC terms  $\boldsymbol{\Omega}_{D(R)}^h$  are given in Eqs. (1) and (2). To facilitate the understanding of the effective magnetic field from these SOC terms, we plot the in-plane components around an arbitrary equal-energy surface under the cancellation gate voltage  $E_z^y$  [Eq. (3)] in Fig. 1. It is shown that the Dresselhaus term almost completely cancels with the Rashba one, leading to a strong suppression of the total in-plane effective magnetic field.

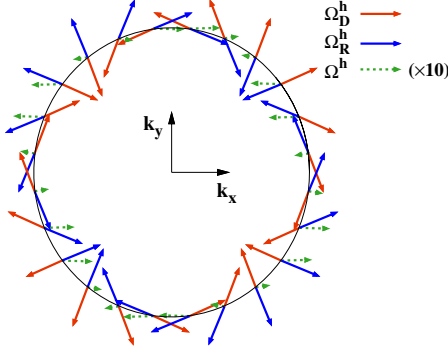


FIG. 1: (Color online) Schematic of the in-plane effective magnetic fields of the lowest HH subband in (111) GaAs/AlAs QWs around an arbitrary equal-energy surface. Red (blue) arrows stand for in-plane components of the Dresselhaus (Rashba) term  $\Omega_{D(R)}^h$  and green arrows represent the sum of the Dresselhaus and Rashba terms  $\Omega_h$ , with its amplitude enlarged by 10 for clarity at the cancellation gate voltage  $E_z^y$ .

Similarly, the effective Hamiltonian of the lowest hole subband in (111) GaAs/InP QWs reads

$$H_{\text{eff}}^l = \varepsilon_{\mathbf{k}}^l + (\boldsymbol{\Omega}_D^l + \boldsymbol{\Omega}_R^l) \cdot \frac{\boldsymbol{\sigma}}{2}, \quad (9)$$

in which  $\varepsilon_{\mathbf{k}}^l = \frac{\hbar^2 \mathbf{k}^2}{2m_t^l}$  and  $m_t^l$  stands for the in-plane effective mass with its form given in Appendix A. The Dresselhaus and Rashba SOC terms  $\boldsymbol{\Omega}_{D(R)}^l$  of the LH are given in Eqs. (4) and (5).

We then construct the microscopic KSBES<sup>5,12</sup> to study the hole spin relaxations in GaAs/AlAs and GaAs/InP QWs, respectively. The KSBES read<sup>5,12</sup>

$$\dot{\rho}_{\mathbf{k},\sigma\sigma'} = \dot{\rho}_{\mathbf{k},\sigma\sigma'}|_{\text{coh}} + \dot{\rho}_{\mathbf{k},\sigma\sigma'}|_{\text{scat}}, \quad (10)$$

where  $\rho_{\mathbf{k},\sigma\sigma'}$  represent the density matrix elements of holes with the diagonal ones  $\rho_{\mathbf{k},\sigma\sigma} \equiv f_{\mathbf{k}\sigma}$  ( $\sigma = \pm 1/2$ ) describing the distribution functions and the off-diagonal ones  $\rho_{\mathbf{k},1/2-1/2} = \rho_{\mathbf{k},-1/2\ 1/2}^* \equiv \rho_{\mathbf{k}}$  denoting the spin coherence.  $\dot{\rho}_{\mathbf{k},\sigma\sigma'}|_{\text{coh}}$  are the coherent terms describing the coherent spin precession due to the effective magnetic field from both the Dresselhaus and Rashba terms while the Hartree-Fock Coulomb interaction is neglected due to

the small spin polarization.<sup>5</sup> Their expressions are given by

$$\left. \frac{\partial f_{\mathbf{k},\sigma}}{\partial t} \right|_{\text{coh}} = -2\sigma[\Omega_x(\mathbf{k})\text{Im}\rho_{\mathbf{k}} + \Omega_y(\mathbf{k})\text{Re}\rho_{\mathbf{k}}], \quad (11)$$

$$\left. \frac{\partial \rho_{\mathbf{k}}}{\partial t} \right|_{\text{coh}} = \frac{1}{2}[i\Omega_x(\mathbf{k}) + \Omega_y(\mathbf{k})](f_{\mathbf{k}1/2} - f_{\mathbf{k}-1/2}) - i\Omega_z(\mathbf{k})\rho_{\mathbf{k}}. \quad (12)$$

Here,  $\Omega_i$  ( $i = x, y, z$ ) are the three components of the effective magnetic field from both the Dresselhaus and Rashba terms.  $\dot{\rho}_{\mathbf{k},\sigma\sigma'}|_{\text{scat}}$  are the scattering terms including the spin conserving ones, i.e., the hole-hole ( $V_{\mathbf{q}}^2$ ), hole-impurity ( $U_{\mathbf{q}}^2$ ), hole-acoustic-phonon ( $|M_{\mathbf{Q},\text{AC}}|^2$ ), polar hole-longitudinal-optical-phonon ( $|M_{\mathbf{Q},\text{LO}}^{\text{polar}}|^2$ ) and non-polar hole-optical-phonon ( $|M_{\mathbf{Q},\lambda}^{\text{nonp}}|^2$ ) scatterings with  $\lambda = \text{LO/TO}$  denoting longitudinal-optical/transverse-optical phonon and the spin-flip ones due to the EY mechanism.<sup>44</sup> Their detailed expressions can be found in Ref. 48 (Note the scatterings in Ref. 48 are given in bulk and one needs to transform them to two-dimensional cases). The scattering matrix elements  $V_{\mathbf{q}}^2 = \left(\frac{\sum_{q_z} v_Q |I(iq_z)|^2}{\epsilon(\mathbf{q})}\right)^2$  and  $U_{\mathbf{q}}^2 = \sum_{q_z} [Z_i v_Q / \epsilon(\mathbf{q})]^2 |I(iq_z)|^2$ , with  $Z_i$  being the charge number of the impurity (assumed to be 1 in our calculation).<sup>23</sup>  $\epsilon(\mathbf{q}) = 1 - \sum_{q_z} v_Q |I(iq_z)|^2 \sum_{\mathbf{k},\sigma} \frac{f_{\mathbf{k}+\mathbf{q},\sigma} - f_{\mathbf{k},\sigma}}{\epsilon_{\mathbf{k}+\mathbf{q}} - \epsilon_{\mathbf{k}}}$  stands for the screening under random phase approximation;<sup>49</sup> the bare Coulomb potential  $v_Q = \frac{4\pi e^2}{Q^2}$  with  $Q^2 = \mathbf{q}^2 + q_z^2$ ; and the form factor  $|I(iq_z)|^2 = \pi^4 \sin^2 y / [y^2 (y^2 - \pi^2)^2]$  with  $y = q_z a/2$ .  $|M_{\mathbf{Q},\text{LO}}^{\text{polar}}|^2 = [2\pi e^2 \omega_{\text{LO}} / (\mathbf{q}^2 + q_z^2)] (\kappa_{\infty}^{-1} - \kappa_0^{-1}) |I(iq_z)|^2$  with  $\omega_{\text{LO}}$  denoting the LO phonon energy and  $\kappa_0$  ( $\kappa_{\infty}$ ) being the static (optical) dielectric constant.<sup>16</sup>  $|M_{\mathbf{Q},\lambda}^{\text{nonp}}|^2 = \frac{3\hbar d_0^2}{2d\omega_{\lambda} a_{\text{GaAs}}^2} |I(iq_z)|^2$  for the nonpolar HH-optical-phonon scatterings and  $|M_{\mathbf{Q},\lambda}^{\text{nonp}}|^2 = \frac{\eta \hbar d_0^2}{2d\omega_{\lambda} a_{\text{GaAs}}^2} |I(iq_z)|^2$  for the nonpolar LH-optical-phonon ones with  $d_0$ ,  $d$ ,  $a_{\text{GaAs}}$ , and  $\omega_{\text{TO}}$  representing the optical deformation potential,<sup>50</sup> the mass density,<sup>23</sup> the lattice constant of GaAs,<sup>42</sup> and the TO phonon energy,<sup>45</sup> respectively.  $\eta = 1(5)$  for  $\lambda = \text{LO}(\text{TO})$ . The matrix element for the hole-acoustic phonon scattering due to the deformation potential reads  $|M_{\mathbf{Q},\text{AC}}^{\text{def}}|^2 = \frac{\hbar \Xi^2 Q}{2dv_{\text{sl}}} |I(iq_z)|^2$  with  $\Xi$  denoting the deformation potential and  $v_{\text{sl}}$  being the velocity of the longitudinal sound wave.<sup>23</sup> For the hole-acoustic phonon scattering due to the piezoelectric coupling,  $|M_{\mathbf{Q},\text{AC}}^{\text{pl}}|^2 = \frac{32\pi^2 \hbar e^2 e_{14}^2 (3q_x' q_y' q_z')^2}{\kappa_0^2 dv_{\text{sl}} Q^7} |I(iq_z)|^2$  for the longitudinal phonon and  $|M_{\mathbf{Q},\text{AC}}^{\text{pt}}|^2 = \frac{32\pi^2 \hbar e^2 e_{14}^2}{\kappa_0^2 dv_{\text{st}} Q^5} [q_x'^2 q_y'^2 + q_y'^2 q_z'^2 + q_z'^2 q_x'^2 - \frac{(3q_x' q_y' q_z')^2}{Q^2}] |I(iq_z)|^2$  for the transverse phonon, where  $q_x' = \frac{1}{\sqrt{6}} q_x - \frac{1}{\sqrt{2}} q_y + \frac{1}{\sqrt{3}} q_z$ ,  $q_y' = \frac{1}{\sqrt{6}} q_x + \frac{1}{\sqrt{2}} q_y + \frac{1}{\sqrt{3}} q_z$  and  $q_z' = -\frac{2}{\sqrt{6}} q_x + \frac{1}{\sqrt{3}} q_z$ .  $v_{\text{st}}$  represents the velocity of the transverse sound wave and  $e_{14}$  is the piezoelectric constant.<sup>23</sup> The spin mixing  $\hat{\Lambda}_{\mathbf{k},\mathbf{k}'}$  for the lowest HH and

TABLE I: Parameters used in the calculation (from Ref. 42 unless otherwise specified)

$\gamma_1$	6.85	$\gamma_2$	2.10	$\gamma_3$	2.90
$b_{41}$	$-81.93 \text{ eV}\text{\AA}^3$	$b_{42}$	$1.47 \text{ eV}\text{\AA}^3$	$b_{51}$	$0.49 \text{ eV}\text{\AA}^3$
$b_{52}$	$-0.98 \text{ eV}\text{\AA}^3$	$D'_u$	4.67 eV	$a_{\text{GaAs}}$	5.65 \text{\AA}
$a_{\text{AlAs}}$	5.66 \text{\AA}	$a_{\text{InP}}$	5.87 \text{\AA}	$C_{11}$	11.81
$C_{12}$	5.32	$C_{44}$	5.94	$d$	$5.31 \text{ g/cm}^3$
$d_0$	48 eV <sup>a</sup>	$\omega_{\text{LO}}$	35.4 meV <sup>b</sup>	$\omega_{\text{TO}}$	33.2 meV <sup>b</sup>
$e_{14}$	$1.41 \times 10^9 \text{ V/m}^c$	$\kappa_\infty$	10.8 <sup>c</sup>	$\Xi$	8.5 eV <sup>c</sup>
$v_{\text{sl}}$	$5.29 \times 10^3 \text{ m/s}^c$	$v_{\text{st}}$	$2.48 \times 10^3 \text{ m/s}^c$	$\kappa_0$	12.9 <sup>c</sup>

<sup>a</sup>Reference 50

<sup>b</sup>Reference 16

<sup>c</sup>Reference 23

LH subbands in the spin-flip scattering terms are detailed in Appendix C.

### III. NUMERICAL RESULTS

We present our results obtained by numerically solving the KSBEs. All the parameters used in our calculation are listed in Table I. The initial spin polarization is along the QW growth direction except otherwise specified. We set the initial spin polarization as 2.5 %. Note that the SRT is insensitive to the small spin polarization.<sup>16</sup> It is noted that the system is always in the strong scattering limit in the present investigation.

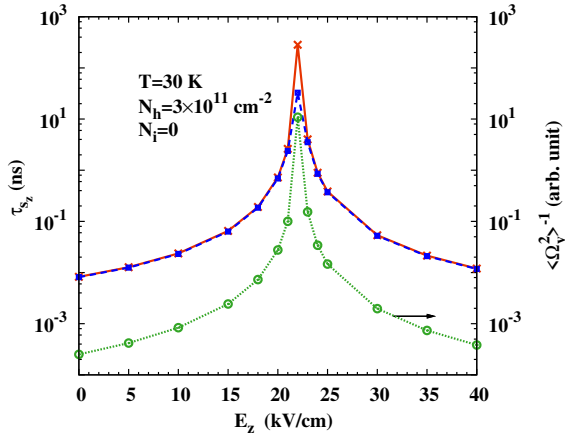


FIG. 2: (Color online) HH SRT along the  $z$ -axis  $\tau_{sz}$  and the inverse of the inhomogeneous broadening  $\langle \Omega_y^2 \rangle^{-1}$  of the lowest hole subband in (111) GaAs/AlAs QWs against the gate voltage  $E_z$ . Red solid (blue dashed) curve represents the SRT due to the DP (both DP and EY) mechanism. The temperature  $T = 30 \text{ K}$ , the hole density  $N_h = 3 \times 10^{11} \text{ cm}^{-2}$  and the impurity density  $N_i = 0$ . Note the scale of  $\langle \Omega_y^2 \rangle^{-1}$  is on the right-hand side of the frame.

#### A. HH spin relaxation in GaAs/AlAs QWs

Before a full investigation by numerically solving the KSBEs, we start from an analytical analysis of the DP spin relaxation of the lowest hole subband, which is HH like, in (111) GaAs/AlAs QWs. In the strong scattering limit, the evolution of spin polarization along the  $z$ -axis can be approximated by<sup>51</sup>

$$\dot{S}_z = -\tau_p^* [S_z \langle \Omega_x^2 + \Omega_y^2 \rangle - S_x \langle \Omega_x \Omega_z \rangle - S_y \langle \Omega_y \Omega_z \rangle], \quad (13)$$

with  $\tau_p^*$  standing for the effective momentum scattering time contributed by the hole-hole, hole-impurity and hole-phonon scatterings.<sup>16,43</sup> The evolutions of the in-plane components  $S_x$  and  $S_y$  can be obtained by index permutation. It is noted that unlike (001) III-V zincblende QWs where  $\Omega_z$  is absent and the inhomogeneous broadening of the spin polarization along the  $z$ -axis is determined by  $\langle \Omega_\perp^2 \rangle = \langle \Omega_x^2 + \Omega_y^2 \rangle$ ,<sup>5</sup> for (111) QWs,  $\Omega_z$  and  $\langle \Omega_x \Omega_z \rangle$  are nonzero under the effective magnetic field from both the Dresselhaus and Rashba terms given in Eqs. (1) and (2). This makes the evolutions more complex compared with (001) QWs, i.e.,

$$\dot{S}_z = -\tau_p^* [S_z \langle \Omega_x^2 + \Omega_y^2 \rangle - S_x \langle \Omega_x \Omega_z \rangle], \quad (14)$$

$$\dot{S}_x = -\tau_p^* [S_x \langle \Omega_y^2 + \Omega_z^2 \rangle - S_z \langle \Omega_x \Omega_z \rangle], \quad (15)$$

$$\dot{S}_y = -\tau_p^* [S_y \langle \Omega_x^2 + \Omega_z^2 \rangle]. \quad (16)$$

The exact solutions are given in Appendix D. Specially by setting the initial spin polarization along the  $z$ -axis as  $S_z(0)$ , we obtain  $S_z = S_z(0)e^{-t/\tau_{sz}}$  approximately by considering that  $\langle \Omega_x^2 \rangle$ ,  $\langle \Omega_y^2 \rangle$  and  $\langle \Omega_x \Omega_z \rangle$  are much smaller than  $\langle \Omega_z^2 \rangle$  in our investigation. The SRT along the  $z$ -axis reads

$$\tau_{sz} = \tau_p^{*-1} \langle \Omega_y^2 \rangle^{-1}, \quad (17)$$

with  $\langle \Omega_y^2 \rangle$  being the inhomogeneous broadening. This inhomogeneous broadening is unique in (111) QWs and has not been reported in the literature.

We then numerically calculate the spin relaxation of the lowest hole subband, which is HH like, in (111) GaAs/AlAs QWs where the well width is chosen to be 8 nm. We first investigate the SRT due to the DP mechanism and plot the gate-voltage dependence of the SRT along the  $z$ -axis at  $T = 30 \text{ K}$  with the hole density  $N_h = 3 \times 10^{11} \text{ cm}^{-2}$  by red solid curve in Fig. 2. It is seen that the SRT can be effectively modulated by the gate voltage and a peak appears at  $E_z \approx 22 \text{ kV/cm}$ . Under this gate voltage, the SRT is as long as 283 ns which is about four orders of magnitude larger than the one without any bias. This peak results from the suppression of the inhomogeneous broadening  $\langle \Omega_y^2 \rangle$  as shown by green dotted curve in Fig. 2. This suppression originates from the cancellation of the  $y$ -component of the effective magnetic field  $\Omega_y$  [Eq. (3)].

Since the suppression of the DP spin relaxation is determined by the cancellation of the  $y$ -component of the

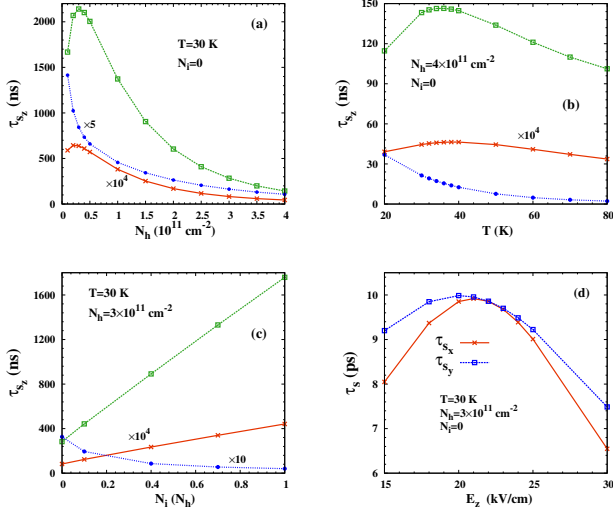


FIG. 3: (Color online) HH SRT along the  $z$ -axis  $\tau_{sz}$  of the lowest hole subband in (111) GaAs/AlAs QWs as a function of (a) the hole density with temperature  $T = 30$  K and impurity density  $N_i = 0$ ; (b) temperature with the hole density  $N_h = 4 \times 10^{11} \text{ cm}^{-2}$  and  $N_i = 0$ ; and (c) impurity density with  $T = 30$  K and  $N_h = 3 \times 10^{11} \text{ cm}^{-2}$ . Red curves with  $\times$  stand for the SRTs due to the DP mechanism under zero bias. Green curves with  $\square$  (blue ones with  $\bullet$ ) represent the SRTs due to the DP (both DP and EY) mechanism at the cancellation gate voltage  $E_z = 22 \text{ kV/cm}$ . (d) HH SRT along the  $x$  ( $y$ )-axis  $\tau_{sx}$  ( $\tau_{sy}$ ) against the gate voltage  $E_z$  with  $T = 30$  K,  $N_h = 3 \times 10^{11} \text{ cm}^{-2}$  and  $N_i = 0$ .

effective magnetic field  $\Omega_y$  [Eq. (3)], it is robust against the hole density, temperature and impurity density. In Fig. 3(a)-(c), we plot the hole density, temperature and impurity density dependences of the SRT under zero bias and the cancellation gate voltage  $E_z = 22 \text{ kV/cm}$  as red curves with  $\times$  and green ones with  $\square$ , respectively. It is shown that the SRT at the cancellation gate voltage is always four orders of magnitude larger than the one under zero bias. In addition, we also observe peaks in the hole density and temperature dependences with the peak locations fixed under different gate voltages. The peak in the density dependence of the SRT has been theoretically predicted by Jiang and Wu<sup>48</sup> and experimentally confirmed<sup>52–55</sup> recently, which is attributed to the crossover from the nondegenerate to degenerate limit. The peak in the temperature dependence of the SRT was predicted by Zhou *et al.*<sup>23</sup> and experimentally realized by Leyland *et al.*,<sup>56</sup> Ruan *et al.*,<sup>57</sup> and Han *et al.*,<sup>54</sup> which is solely caused by the Coulomb scattering.<sup>23</sup> The location of the peak is insensitive to the gate voltage just the same as the case for electrons in (111) QWs.<sup>38</sup>

It is further noted that the EY mechanism is usually the major mechanism in hole spin relaxation in bulk GaAs.<sup>45</sup> In order to rule out the influence of the EY mechanism to the predicted phenomena, we plot in Fig. 2 the gate-voltage dependence of the SRT due to both the DP and EY mechanisms as the blue dashed curve. It

is seen that the EY mechanism can be important only around the cancellation gate voltage where the DP spin relaxation is greatly suppressed. Away from the cancellation gate voltage, the contribution of the EY mechanism is negligible since the spin mixing between the HH and LH is extremely small due to the large energy splitting between the HH and LH subbands in QWs with small well width. Moreover, since the EY mechanism is important at the cancellation gate voltage, we also plot in Fig. 3(a)(c) the hole density, temperature and impurity density dependences of the SRT due to both the EY and DP mechanisms under this gate voltage (blue curves with  $\bullet$ ). We find that the peaks in the hole density and temperature dependences disappear since the SRT caused by the EY mechanism decreases with the hole density and temperature.<sup>3,5,45</sup> Moreover, the SRT due to the EY mechanism also decreases with the impurity density.<sup>3,5,45</sup> However, away from the cancellation field, the spin relaxation is determined by the DP mechanism only and the peaks still exist in the corresponding temperature and density dependences.

Finally, we address the anisotropy of the spin relaxation with respect to the spin polarization direction. The SRT along the  $z$ -axis  $\tau_{sz}$  is given in Eq. (17). Similarly, one obtains the SRTs along the  $x$ - and  $y$ -axes as

$$\tau_{sx} = \tau_p^{*-1} \langle \Omega_x^2 + \Omega_y^2 + \Omega_z^2 \rangle^{-1}, \quad (18)$$

$$\tau_{sy} = \tau_p^{*-1} \langle \Omega_x^2 + \Omega_z^2 \rangle^{-1}, \quad (19)$$

by setting the initial spin polarizations along the  $x$ - and  $y$ -axes correspondingly. By comparing Eq. (17) with Eqs. (18) and (19), one finds a strong anisotropy between the out-of- and in-plane spin relaxation, since  $\Omega_z$  is about one order of magnitude larger than the in-plane components  $\Omega_x$  and  $\Omega_y$  in (111) QWs with small well width. In addition, a marginal anisotropy also arises between the in-plane spin relaxations from Eqs. (18) and (19). The numerical result of the SRT along the  $x$  ( $y$ )-axis  $\tau_{sx}$  ( $\tau_{sy}$ ) is shown in Fig. 3(d) by red curve with  $\times$  (blue one with  $\square$ ). One finds from the figure that both  $\tau_{sx}$  and  $\tau_{sy}$  are about two orders of magnitude smaller than  $\tau_{sz}$ .

## B. LH spin relaxation in GaAs/InP QWs

We also investigate the spin relaxation of the lowest hole subband, which is LH like, in (111) GaAs/InP QWs with the well width  $a = 20 \text{ nm}$ . The gate-voltage dependence of the SRT along the  $z$ -axis due to the DP mechanism under different temperatures is shown in Fig. 4 and a peak is also observed. We find that the peak becomes less pronounced than that in GaAs/AlAs QWs since the cancellation only occurs on a special momentum circle in GaAs/InP QWs.<sup>38</sup> In addition, when the temperature increases, the peak location changes, similar to the case for electrons in (111) GaAs QWs.<sup>38</sup> It is noted that the contribution of the EY mechanism is in the order of 10 ns and is therefore always negligible in this case.



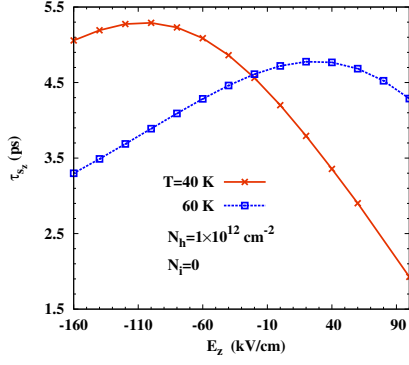


FIG. 4: (Color online) LH SRT along the  $z$ -axis  $\tau_{s_z}$  of the lowest hole subband in (111) GaAs/InP QWs against the gate voltage  $E_z$ . Red curve with  $\times$  (blue one with  $\square$ ) stands for the case with temperature  $T = 40$  (60) K. The hole density  $N_h = 1 \times 10^{12} \text{ cm}^{-2}$  and impurity density  $N_i = 0$ .

#### IV. SUMMARY

In summary, we have investigated the hole spin relaxations in  $p$ -type (111) GaAs/AlAs and GaAs/InP QWs with only the lowest hole subband being relevant. The lowest hole subband is HH like in the former case while LH like in the latter one. In both systems, we utilize the subband Löwdin perturbation method to obtain the effective Hamiltonian including the Dresselhaus and Rashba SOC. Under a proper gate voltage, the total in-plane effective magnetic field in (111) GaAs/AlAs QWs can be strongly suppressed in the whole momentum space, while the one in (111) GaAs/InP QWs can only be suppressed to zero on a special momentum circle. Therefore, tuning the gate voltage is an efficient way to modulate the hole spin relaxation in (111) QWs.

We calculate the hole spin relaxation due to the DP and EY mechanisms by numerically solving the KS-BEs with all the relevant scatterings explicitly included. For (111) GaAs/AlAs QWs, the contribution of the EY mechanism is negligible unless the DP mechanism is strongly suppressed. In addition, we predict a pronounced peak in the gate voltage-dependence of the HH SRT where an extremely long SRT (upto hundreds of nanoseconds) can be reached. This peak comes from the suppression of the unique inhomogeneous broadening in (111) GaAs/AlAs QWs, specifically, the cancellation of the  $y$ -component of the effective magnetic field. The suppression of the spin relaxation is robust against the hole density, temperature and impurity density. A strong anisotropy between the out-of- and in-plane spin relaxations is also addressed. In (111) GaAs/InP QWs, a peak is also predicted in the gate-voltage dependence of the LH SRT. However, the peak becomes less pronounced compared with the case in (111) GaAs/AlAs QWs since the cancellation only occurs on a special momentum circle in GaAs/InP QWs. The contribution of the EY mechanism is always negligible in this case. This investigation

suggests that the HH in (111) GaAs/AlAs QWs offers unique properties for the spintronic devices and calls for experimental investigations.

#### Acknowledgments

This work was supported by the National Basic Research Program of China under Grant No. 2012CB922002 and the National Natural Science Foundation of China under Grant No. 10725417.

#### Appendix A: EFFECTIVE MASS AND SPIN-ORBIT COUPLING COEFFICIENTS

The in-plane effective mass  $m_t^h$  in Eq. (8) and the Dresselhaus (Rashba) strengths  $\beta_i^h$  ( $\alpha_i^h$ ) ( $i = x, y, z$ ) of the lowest hole subband, which is HH like, in Eqs. (1) and (2) are given by

$$\frac{1}{m_t^h} = \frac{\gamma_1 + \gamma_3}{m_0} - \sum_{n_z \neq 1} \frac{2B_1^2 Q_{1n_z}^2}{\hbar^2 \Delta_{n_z 1}^{lh}} - \frac{2C_1^2}{\hbar^2 \Delta_{11}^{lh}}, \quad (\text{A1})$$

$$\beta_x^h = \frac{b_{42}}{\sqrt{3}} - \frac{4(C_1 B_3 + B_2 C_3)}{\Delta_{11}^{lh}} + \sum_{n_z \neq 1} \frac{4(B_1 C_4 + 2C_2 B_2) Q_{1n_z}^2}{\Delta_{n_z 1}^{lh}}, \quad (\text{A2})$$

$$\beta_y^h = \frac{-b_{51} + b_{52}}{\sqrt{3}} + \frac{4(C_1 B_3 - B_2 C_3)}{\Delta_{11}^{lh}} + \sum_{n_z \neq 1} \frac{4(2C_2 B_2 - B_1 C_4) Q_{1n_z}^2}{\Delta_{n_z 1}^{lh}}, \quad (\text{A3})$$

$$\beta_z^h = -\frac{\sqrt{6}}{2} b_{41} - \frac{23\sqrt{6}}{24} b_{42} + \frac{4(C_3 B_3 - C_1 B_2)}{\Delta_{11}^{lh}} + \sum_{n_z \neq 1} \frac{4(B_1 C_2 - 2B_2 C_4) Q_{1n_z}^2}{\Delta_{n_z 1}^{lh}}, \quad (\text{A4})$$

$$\alpha_x^h = \sum_{n_z \neq 1} \frac{4P_{1n_z} Q_{1n_z}}{\Delta_{n_z 1}^{lh} \Delta_{n_z 1}^{hh}} (B_1 B_3 - C_1 C_4 n_z^2 + 2B_2^2 - C_2 C_3 n_z^2) + \sum_{n_z \neq 1} \frac{4P_{1n_z} Q_{1n_z}}{\Delta_{11}^{lh}} \left( \frac{1}{\Delta_{n_z 1}^{lh}} - \frac{1}{\Delta_{n_z 1}^{hh}} \right) \times (B_1 B_3 - C_1 C_4 + 2B_2^2 - C_2 C_3), \quad (\text{A5})$$

$$\alpha_y^h = \sum_{n_z \neq 1} \frac{4P_{1n_z} Q_{1n_z}}{\Delta_{n_z 1}^{lh} \Delta_{n_z 1}^{hh}} (B_1 B_3 - C_1 C_4 n_z^2 - 2B_2^2 + C_2 C_3 n_z^2) + \sum_{n_z \neq 1} \frac{4P_{1n_z} Q_{1n_z}}{\Delta_{11}^{lh}} \left( \frac{1}{\Delta_{n_z 1}^{lh}} - \frac{1}{\Delta_{n_z 1}^{hh}} \right) \times (B_1 B_3 - C_1 C_4 - 2B_2^2 + C_2 C_3), \quad (\text{A6})$$

$$\begin{aligned}\alpha_z^h = & \sum_{n_z \neq 1} \frac{4P_{1n_z}Q_{1n_z}}{\Delta_{n_z1}^{lh}\Delta_{n_z1}^{hh}}(B_1B_2 - C_1C_2n_z^2 - 2B_2B_3 \\ & + C_3C_4n_z^2) + \sum_{n_z \neq 1} \frac{4P_{1n_z}Q_{1n_z}}{\Delta_{11}^{lh}}\left(\frac{1}{\Delta_{n_z1}^{lh}} - \frac{1}{\Delta_{n_z1}^{hh}}\right) \\ & \times (B_1B_2 - C_1C_2 - 2B_2B_3 + C_3C_4). \quad (\text{A7})\end{aligned}$$

The in-plane effective mass  $m_t^l$  in Eq. (9), the Dresselhaus strengths  $\beta_x^{l1,l2}$ ,  $\beta_z^l$  and the Rashba strengths  $\alpha_{x,z}^l$  of the lowest hole subband, which is LH like, in Eqs. (4) and (5) read

$$\begin{aligned}\frac{1}{m_t^l} = & \frac{\gamma_1 - \gamma_3}{m_0} - \frac{2(C_1^2 + C_3^2)}{\hbar^2 \Delta_{11}^{hl}} - \sum_{n_z \neq 1} \frac{2}{\hbar^2 \Delta_{n_z1}^{hl}} \\ & \times (B_1^2 + 4B_2^2)Q_{1n_z}^2, \quad (\text{A8})\end{aligned}$$

$$\begin{aligned}\beta_x^{l1} = & \frac{4b_{41} + 7b_{42}}{4\sqrt{3}} - \frac{\sqrt{3}}{2}(b_{51} + b_{52}) - \frac{4}{\Delta_{11}^{hl}}(B_2C_3 \\ & - C_1B_3) + \sum_{n_z \neq 1} \frac{4(-B_1C_4 + 2C_2B_2)Q_{1n_z}^2}{\Delta_{n_z1}^{hl}} \quad (\text{A9})\end{aligned}$$

$$\beta_x^{l2} = -\frac{4\sqrt{3}b_{41}}{3} - \frac{7\sqrt{3}b_{42}}{3} - \sqrt{3}b_{52}, \quad (\text{A10})$$

$$\begin{aligned}\beta_z^l = & -\frac{\sqrt{6}b_{41}}{6} - \frac{13\sqrt{6}b_{42}}{24} - \frac{4(C_1B_2 + C_3B_3)}{\Delta_{11}^{hl}} \\ & + \sum_{n_z \neq 1} \frac{4(B_1C_2 + 2B_2C_4)Q_{1n_z}^2}{\Delta_{n_z1}^{hl}}, \quad (\text{A11})\end{aligned}$$

$$\begin{aligned}\alpha_x^l = & \sum_{n_z \neq 1} \frac{4P_{1n_z}Q_{1n_z}}{\Delta_{n_z1}^{ll}\Delta_{n_z1}^{hl}}(B_1B_3 - C_1C_4n_z^2 - 2B_2^2 \\ & + C_2C_3n_z^2) + \sum_{n_z \neq 1} \frac{4P_{1n_z}Q_{1n_z}}{\Delta_{11}^{ll}}\left(\frac{1}{\Delta_{n_z1}^{hl}} - \frac{1}{\Delta_{n_z1}^{ll}}\right) \\ & \times (B_1B_3 - C_1C_4 - 2B_2^2 + C_2C_3), \quad (\text{A12})\end{aligned}$$

$$\begin{aligned}\alpha_z^l = & -\sum_{n_z} \frac{4W_1P_{1n_z}Q_{1n_z}}{\Delta_{11}^{hl}\Delta_{n_z1}^{hl}} - \sum_{n_z \neq 1} \frac{4W_1P_{1n_z}Q_{1n_z}n_z^2}{\Delta_{n_z1}^{ll^2}} \\ & - \sum_{n_z \neq 1} \frac{4P_{1n_z}Q_{1n_z}}{\Delta_{n_z1}^{ll}\Delta_{11}^{hl}}(-B_1B_2 + C_1C_2 - 2B_2B_3 \\ & + C_3C_4) + \sum_{n_z \neq 1} \frac{4P_{1n_z}Q_{n_z1}}{\Delta_{n_z1}^{ll}\Delta_{n_z1}^{hl}}(B_1B_2 - C_1C_2n_z^2 \\ & + 2B_2B_3 - C_3C_4n_z^2). \quad (\text{A13})\end{aligned}$$

In above equations,  $\gamma_i$  are Kohn-Luttinger parameters;  $b_{41,42,51,52}$  stand for the coefficients of the Dresselhaus SOC of the valence band;  $\Delta_{n_1n_2}^{hh}$  ( $\Delta_{n_1n_2}^{ll}$ ) is the energy difference between  $n_1$ -th and  $n_2$ -th subbands of HH (LH);  $\Delta_{n_1n_2}^{hl}$  is the energy difference between  $n_1$ -th HH and  $n_2$ -th LH subbands.  $B_1 = \frac{\sqrt{3}\hbar^2(2\gamma_2+\gamma_3)}{3m_0}$ ,  $B_2 = \frac{\sqrt{6}\hbar^2(-\gamma_2+\gamma_3)}{6m_0}$ , and  $B_3 = \frac{\sqrt{3}\hbar^2(\gamma_2+2\gamma_3)}{6m_0}$ .  $C_1 = (b_{41} + \frac{9}{4}b_{42} - \frac{1}{2}b_{52})\frac{\pi^2}{a^2}$ ,  $C_2 = \frac{\sqrt{2}}{4}(b_{41} + \frac{9}{4}b_{42} - b_{51} + b_{52})$ ,  $C_3 = \frac{\sqrt{2}\pi^2}{4a^2}(2b_{42} + b_{52})$ , and

$$\begin{aligned}C_4 = & \frac{1}{4}(b_{42} + b_{51} - b_{52}). \quad P_{n_1n_2} = \frac{4an_1n_2[(-1)^{n_1+n_2}-1]}{(n_1^2-n_2^2)^2\pi^2}(1 - \\ & \delta_{n_1,n_2}), \quad Q_{n_1n_2} = \frac{2n_1n_2[(-1)^{n_1+n_2}-1]}{(n_1^2-n_2^2)a}(\delta_{n_1,n_2}-1), \text{ and } W_1 = \\ & \frac{3\sqrt{2}\pi^2}{a^2}(\frac{1}{6}b_{41} + \frac{7}{24}b_{42} + \frac{1}{4}b_{51} - \frac{1}{4}b_{52})(\frac{2}{3}b_{41} + \frac{7}{6}b_{42} + \frac{1}{2}b_{52}).\end{aligned}$$

## Appendix B: LUTTINGER HAMILTONIAN FOR (111)-ORIENTED III-V ZINC-BLENDE CRYSTAL

The Luttinger Hamiltonian  $H_L$ , the Dresselhaus SOC  $H_{8v8v}^b$  and the strain Hamiltonian  $H_\epsilon$  in Eq. (6) are given in the following. The Luttinger Hamiltonian  $H_L$  can be written as<sup>46</sup>

$$H_L = \begin{pmatrix} F & H & I & 0 \\ H^* & G & 0 & I \\ I^* & 0 & G & -H \\ 0 & I^* & -H^* & F \end{pmatrix} \quad (\text{B1})$$

in the basis of the eigenstates of  $J_z$  with eigenvalues  $\frac{3}{2}, \frac{1}{2}, -\frac{1}{2}$ , and  $-\frac{3}{2}$  in sequence, where  $F = \frac{\hbar^2}{2m_0}[(\gamma_1 + \gamma_3)(k_x^2 + k_y^2) + (\gamma_1 - 2\gamma_3)k_z^2]$ ,  $G = \frac{\hbar^2}{2m_0}[(\gamma_1 - \gamma_3)(k_x^2 + k_y^2) + (\gamma_1 + 2\gamma_3)k_z^2]$ ,  $H = -\frac{\hbar^2}{2m_0}[\frac{\sqrt{6}}{3}(-\gamma_2 + \gamma_3)k_+^2 + \frac{2\sqrt{3}}{3}(2\gamma_2 + \gamma_3)k_-k_z]$ , and  $I = -\frac{\hbar^2}{2m_0}[\frac{\sqrt{3}}{3}(\gamma_2 + 2\gamma_3)k_-^2 + \frac{2\sqrt{6}}{3}(-\gamma_2 + \gamma_3)k_+k_z]$ , with  $k_\pm = k_x \pm ik_y$ .  $H_L^{(0)} = \frac{\hbar^2 k_z^2}{2m_0} \text{diag}(\gamma_1 - 2\gamma_3, \gamma_1 + 2\gamma_3, \gamma_1 + 2\gamma_3, \gamma_1 - 2\gamma_3)$  corresponds to the part of the Luttinger Hamiltonian  $H_L$  by setting  $k_{x,y} = 0$ .

The Dresselhaus SOC  $H_{8v8v}^b$  is given by<sup>42</sup>

$$\begin{aligned}H_{8v8v}^b = & -b_{41}(\{k'_x, k'_y\}^2 - k'_z\}J'_x + \text{cp}) - b_{42}(\{k'_x, k'_y\}^2 \\ & - k'_z\}J'_x + \text{cp}) - b_{51}(\{k'_x, k'_y\}^2 + k'_z\}\{J'_x, J'_y\}^2 \\ & - J'_z\} + \text{cp}) - b_{52}(k'_x\{J'_x, J'_y\}^2 - J'_z\} + \text{cp}), \quad (\text{B2})\end{aligned}$$

where  $k'_x = \frac{1}{\sqrt{6}}k_x - \frac{1}{\sqrt{2}}k_y + \frac{1}{\sqrt{3}}k_z$ ,  $k'_y = \frac{1}{\sqrt{6}}k_x + \frac{1}{\sqrt{2}}k_y + \frac{1}{\sqrt{3}}k_z$ ,  $k'_z = -\frac{2}{\sqrt{6}}k_x + \frac{1}{\sqrt{3}}k_z$ ,  $J'_x = \frac{1}{\sqrt{6}}J_x - \frac{1}{\sqrt{2}}J_y + \frac{1}{\sqrt{3}}J_z$ ,  $J'_y = \frac{1}{\sqrt{6}}J_x + \frac{1}{\sqrt{2}}J_y + \frac{1}{\sqrt{3}}J_z$ , and  $J'_z = -\frac{2}{\sqrt{6}}J_x + \frac{1}{\sqrt{3}}J_z$ .  $J_i$  ( $i = x, y, z$ ) represent the spin-3/2 angular momentum matrices and cp denotes the cyclic permutation of the preceding terms.

The Bir-Pikus strain Hamiltonian  $H_\epsilon$  reads<sup>42,47</sup>

$$H_\epsilon = \text{diag}(-E_S^1, E_S^1, E_S^1, -E_S^1) - E_S^2 I_4, \quad (\text{B3})$$

$$E_S^1 = 2D'_u \epsilon_a, \quad (\text{B4})$$

$$E_S^2 = 3D_d \epsilon_b, \quad (\text{B5})$$

$$\epsilon_a = -\frac{1}{3}(1 + \frac{1}{\sigma^{(111)}})\epsilon_{||}, \quad (\text{B6})$$

$$\epsilon_b = \frac{1}{3}(2 - \frac{1}{\sigma^{(111)}})\epsilon_{||}, \quad (\text{B7})$$

$$\epsilon_{||} = \frac{a_s - a_e}{a_e}, \quad (\text{B8})$$

$$\sigma^{(111)} = \frac{C_{11} + 2C_{12} + 4C_{44}}{2C_{11} + 4C_{12} - 4C_{44}}. \quad (\text{B9})$$

Here,  $D'_u$  and  $D_d$  stand for the deformation potential constants;  $\epsilon_b$  and  $\epsilon_a$  denote the diagonal and off-diagonal components of the strain tensor;  $a_e$  and  $a_s$  represent the lattice constants of epilayer (GaAs) and substrate materials (AlAs/InP); and  $C_{11}$ ,  $C_{12}$  and  $C_{44}$  are the stiffness constants.<sup>42,47</sup>

### Appendix C: SPIN MIXING $\hat{\Lambda}_{\mathbf{k},\mathbf{k}'}$ FOR THE LOWEST HH AND LH SUBBANDS

The spin mixing  $\hat{\Lambda}_{\mathbf{k},\mathbf{k}'}$  in the spin-flip scattering induced by the EY mechanism reads  $\hat{\Lambda}_{\mathbf{k},\mathbf{k}'} = \hat{I} - \frac{1}{2} \sum_{n_z} (S_{\mathbf{k}}^{(1)} S_{\mathbf{k}'}^{(1)\dagger} - 2S_{\mathbf{k}}^{(1)} S_{\mathbf{k}'}^{(1)\dagger} + S_{\mathbf{k}'}^{(1)} S_{\mathbf{k}}^{(1)\dagger})$ , with  $\hat{I}$  being a  $2 \times 2$  unit matrix. For the lowest hole subband, which is HH like, in GaAs/AlAs QWs,  $S_{\mathbf{k}}^{(1)}$  is given by

$$S_{\mathbf{k}}^{(1)} = \begin{pmatrix} 0 & -\frac{H_{14}^{1n_z}}{\Delta_{1n_z}^{hh}} & -\frac{H_{12}^{1n_z}}{\Delta_{1n_z}^{hh}} & -\frac{H_{13}^{1n_z}}{\Delta_{1n_z}^{hh}} \\ -\frac{H_{41}^{1n_z}}{\Delta_{1n_z}^{hh}} & 0 & -\frac{H_{21}^{1n_z}}{\Delta_{1n_z}^{hh}} & -\frac{H_{31}^{1n_z}}{\Delta_{1n_z}^{hh}} \end{pmatrix}. \quad (\text{C1})$$

$H_{ij}^{1n_z} = \langle 1 | H_{ij} | n_z \rangle$  in which 1 ( $n_z$ ) stands for the first ( $n_z$ -th) subband and  $H_{ij}$  represents the  $i$ -th row and  $j$ -th column of the Hamiltonian matrix  $H_{4 \times 4}$  in Eq. (6).  $\Delta_{1n_z}^{hh}$  is the energy difference between the first and  $n_z$ -th HH subbands and  $\Delta_{1n_z}^{hl}$  is the energy difference between the first HH and  $n_z$ -th LH subbands.

For the lowest hole subband, which is LH like, in

GaAs/InP QWs,  $S_{\mathbf{k}}^{(1)}$  is given by

$$S_{\mathbf{k}}^{(1)} = \begin{pmatrix} 0 & -\frac{H_{23}^{1n_z}}{\Delta_{1n_z}^{lh}} & -\frac{H_{21}^{1n_z}}{\Delta_{1n_z}^{lh}} & -\frac{H_{24}^{1n_z}}{\Delta_{1n_z}^{lh}} \\ -\frac{H_{32}^{1n_z}}{\Delta_{1n_z}^{lh}} & 0 & -\frac{H_{31}^{1n_z}}{\Delta_{1n_z}^{lh}} & -\frac{H_{34}^{1n_z}}{\Delta_{1n_z}^{lh}} \end{pmatrix}, \quad (\text{C2})$$

where  $\Delta_{1n_z}^{lh}$  is the energy difference between the first and  $n_z$ -th LH subbands. It is noted that  $S_{\mathbf{k}'}^{(1)}$  can be obtained by replacing  $\mathbf{k}$  in  $S_{\mathbf{k}}^{(1)}$  with  $\mathbf{k}'$ .

### Appendix D: EXACT SOLUTIONS OF Eqs. (14) TO (16)

$$S_z = S_x(0) \frac{\langle \Omega_x \Omega_z \rangle}{u} (-e^{-\lambda_1 \tau_p^* t} + e^{-\lambda_2 \tau_p^* t}) + \frac{S_z(0)}{2u} [(\langle \Omega_x^2 - \Omega_z^2 \rangle + u) e^{-\lambda_1 \tau_p^* t} + (\langle \Omega_x^2 - \Omega_z^2 \rangle + u) e^{-\lambda_2 \tau_p^* t}], \quad (\text{D1})$$

$$S_x = \frac{S_x(0)}{2u} [(\langle \Omega_x^2 - \Omega_z^2 \rangle + u) e^{-\lambda_1 \tau_p^* t} + (\langle \Omega_x^2 - \Omega_z^2 \rangle + u) e^{-\lambda_2 \tau_p^* t}] + S_z(0) \frac{\langle \Omega_x \Omega_z \rangle}{u} (-e^{-\lambda_1 \tau_p^* t} + e^{-\lambda_2 \tau_p^* t}), \quad (\text{D2})$$

$$S_y = S_y(0) e^{-\langle \Omega_x^2 + \Omega_z^2 \rangle \tau_p^* t}, \quad (\text{D3})$$

with  $\lambda_{1,2} = \frac{1}{2}(\langle \Omega_x^2 + 2\Omega_y^2 + \Omega_z^2 \rangle \pm u)$  and  $u = \langle \Omega_x^2 \rangle + \langle \Omega_z^2 \rangle$ .

- 
- \* Author to whom correspondence should be addressed; Electronic address: mwwu@ustc.edu.cn.
- <sup>1</sup> F. Meier and B. P. Zakharchenya, *Optical Orientation* (North-Holland, Amsterdam, 1984).
  - <sup>2</sup> S. A. Wolf, D. D. Awschalom, R. A. Buhrman, J. M. Daughton, S. von Molnár, M. L. Roukes, A. Y. Chtchelkanova, and D. M. Treger, *Science* **294**, 1488 (2001).
  - <sup>3</sup> *Semiconductor Spintronics and Quantum Computation*, edited by D. D. Awschalom, D. Loss, and N. Samarth (Springer-Verlag, Berlin, 2002); *Spin Physics in Semiconductors*, edited by M. I. D'yakonov (Springer, Berlin, 2008).
  - <sup>4</sup> I. Žutić, J. Fabian, and S. Das Sarma, *Rev. Mod. Phys.* **76**, 323 (2004); J. Fabian, A. Matos-Abiad, C. Ertler, P. Stano, and I. Žutić, *Acta Phys. Slov.* **57**, 565 (2007).
  - <sup>5</sup> M. W. Wu, J. H. Jiang, and M. Q. Weng, *Phys. Rep.* **493**, 61 (2010), and references therein.
  - <sup>6</sup> T. Korn, *Phys. Rep.* **494**, 415 (2010).
  - <sup>7</sup> *Handbook of Spin Transport and Magnetism*, edited by E. Y. Tsymlal and I. Žutić (Chapman & Hall/CRC, Boca Raton, FL, 2011).
  - <sup>8</sup> M. I. D'yakonov and V. I. Perel', *Zh. Eksp. Teor. Fiz.* **60**, 1954 (1971) [*Sov. Phys. JETP* **33**, 1053 (1971)].
  - <sup>9</sup> G. Dresselhaus, *Phys. Rev.* **100**, 580 (1955).
  - <sup>10</sup> Y. A. Bychkov and E. I. Rashba, *J. Phys. C* **17**, 6039 (1984); *Pis'ma Zh. Eksp. Teor. Fiz.* **39**, 66 (1984) [*JETP Lett.* **39**, 78 (1984)].

- <sup>11</sup> N. S. Averkiev and L. E. Golub, *Phys. Rev. B* **60**, 15582 (1999).
- <sup>12</sup> M. W. Wu and H. Metiu, *Phys. Rev. B* **61**, 2945 (2000).
- <sup>13</sup> A. Malinowski, R. S. Britton, T. Grevatt, R. T. Harley, D. A. Ritchie, and M. Y. Simmons, *Phys. Rev. B* **62**, 13034 (2000).
- <sup>14</sup> N. S. Averkiev, L. E. Golub, and M. Willander, *J. Phys.: Condens. Matter* **14**, R271 (2002).
- <sup>15</sup> J. Schliemann, J. C. Egues, and D. Loss, *Phys. Rev. Lett.* **90**, 146801 (2003).
- <sup>16</sup> M. Q. Weng and M. W. Wu, *Phys. Rev. B* **68**, 075312 (2003); M. Q. Weng, M. W. Wu, and L. Jiang, *ibid.* **69**, 245320 (2004).
- <sup>17</sup> J. Kainz, U. Rössler, and R. Winkler, *Phys. Rev. B* **68**, 075322 (2003).
- <sup>18</sup> J. Schliemann and D. Loss, *Phys. Rev. B* **68**, 165311 (2003).
- <sup>19</sup> R. Winkler, *Phys. Rev. B* **69**, 045317 (2004).
- <sup>20</sup> S. I. Erlingsson, J. Schliemann, and D. Loss, *Phys. Rev. B* **71**, 035319 (2005).
- <sup>21</sup> N. S. Averkiev, L. E. Golub, A. S. Gurevich, V. P. Evtikhiev, V. P. Kochereshko, A. V. Platonov, A. S. Shkolnik, and Y. P. Efimov, *Phys. Rev. B* **74**, 033305 (2006).
- <sup>22</sup> J. L. Cheng and M. W. Wu, *J. Appl. Phys.* **99**, 083704 (2006).
- <sup>23</sup> J. Zhou, J. L. Cheng, and M. W. Wu, *Phys. Rev. B* **75**, 045305 (2007); J. Zhou and M. W. Wu, *ibid.* **77**, 075318 (2008).



- (2008).
- <sup>24</sup> M. Ohno and K. Yoh, Phys. Rev. B **75**, 241308(R) (2007).
  - <sup>25</sup> B. Liu, H. Zhao, J. Wang, L. Liu, W. Wang, D. Chen, and H. Zhu, Appl. Phys. Lett. **90**, 112111 (2007).
  - <sup>26</sup> D. Stich, J. H. Jiang, T. Korn, R. Schulz, D. Schuh, W. Wegscheider, M. W. Wu, and C. Schüller, Phys. Rev. B **76**, 073309 (2007).
  - <sup>27</sup> J. D. Koralek, C. P. Weber, J. Orenstein, B. A. Bernevig, S. C. Zhang, S. Mack, and D. D. Awschalom, Nature (London) **458**, 610 (2009).
  - <sup>28</sup> Y. Zhou, J. H. Jiang, and M. W. Wu, New J. Phys. **11**, 113039 (2009).
  - <sup>29</sup> Y. Ohno, R. Terauchi, T. Adachi, F. Matsukura, and H. Ohno, Phys. Rev. Lett. **83**, 4196 (1999).
  - <sup>30</sup> W. H. Lau and M. E. Flatté, J. Appl. Phys. **91**, 8682 (2002).
  - <sup>31</sup> M. W. Wu and M. Kuwata-Gonokami, Solid State Commun. **121**, 509 (2002).
  - <sup>32</sup> O. Z. Karimov, G. H. John, R. T. Harley, W. H. Lau, M. E. Flatté, M. Henini, and R. Airey, Phys. Rev. Lett. **91**, 246601 (2003).
  - <sup>33</sup> K. C. Hall, K. Gündoğdu, E. Altunkaya, W. H. Lau, M. E. Flatté, and T. F. Boggess, Phys. Rev. B **68**, 115311 (2003).
  - <sup>34</sup> S. Döhrmann, D. Hägele, J. Rudolph, M. Bichler, D. Schuh, and M. Oestreich, Phys. Rev. Lett. **93**, 147405 (2004).
  - <sup>35</sup> Y. Zhou and M. W. Wu, Europhys. Lett. **89**, 57001 (2010).
  - <sup>36</sup> X. Cartoixa, D. Z.-Y. Ting, and Y.-C. Chang, Phys. Rev. B **71**, 045313 (2005).
  - <sup>37</sup> I. Vurgaftman and J. R. Meyer, J. Appl. Phys. **97**, 053707 (2005).
  - <sup>38</sup> B. Y. Sun, P. Zhang, and M. W. Wu, J. Appl. Phys. **108**, 093709 (2010);
  - <sup>39</sup> B. Y. Sun and K. Shen, Solid State Commun. **151**, 1322 (2011).
  - <sup>40</sup> A. Balocchi, Q. H. Duong, P. Renucci, B. L. Liu, C. Fontaine, T. Amand, D. Lagarde, and X. Marie, Phys. Rev. Lett. **107**, 136604 (2011).
  - <sup>41</sup> P. O. Löwdin, J. Chem. Phys. **19**, 1396 (1951).
  - <sup>42</sup> R. Winkler, *Spin-orbit Coupling Effects in Two-Dimensional Electron and Hole Systems* (Springer, Berlin, 2003).
  - <sup>43</sup> M. W. Wu and C. Z. Ning, Eur. Phys. J. B **18**, 373 (2000); M. W. Wu, J. Phys. Soc. Jpn. **70**, 2195 (2001).
  - <sup>44</sup> Y. Yafet, Phys. Rev. **85**, 478 (1952); R. J. Elliott, *ibid.* **96**, 266 (1954).
  - <sup>45</sup> K. Shen and M. W. Wu, Phys. Rev. B **82**, 115205 (2010).
  - <sup>46</sup> J. M. Luttinger, Phys. Rev. **102**, 1030 (1956).
  - <sup>47</sup> G. L. Bir and G. E. Pikus, *Symmetry and Strain-Induced Effects in Semiconductors* (Wiley, New York, 1974).
  - <sup>48</sup> J. H. Jiang and M. W. Wu, Phys. Rev. B **79**, 125206 (2009).
  - <sup>49</sup> G. D. Mahan, *Many-Particle Physics* (Plenum, New York, 1990).
  - <sup>50</sup> P. Langot, R. Tommasi, and F. Vallée, Phys. Rev. B **54**, 1775 (1996).
  - <sup>51</sup> G. E. Pikus and A. N. Titkov, *Spin relaxation under optical orientation in semiconductors* in:[1], pp. 73-132.
  - <sup>52</sup> M. Krauß, H. C. Schneider, R. Bratschitsch, Z. Chen, and S. T. Cundiff, Phys. Rev. B **81**, 035213 (2010).
  - <sup>53</sup> J. H. Buß, J. Rudolph, S. Starosielec, A. Schaefer, F. Semond, Y. Cordier, A. D. Wieck, and D. Hägele, Phys. Rev. B **84**, 153202 (2011).
  - <sup>54</sup> L. F. Han, Y. G. Zhu, X. H. Zhang, P. H. Tan, H. Q. Ni, and Z. C. Niu, Nanoscale Res. Lett. **6**, 84 (2011).
  - <sup>55</sup> L. F. Han, X. H. Zhang, H. Q. Ni, and Z. C. Niu, Physica E **43**, 1127 (2011).
  - <sup>56</sup> W. J. H. Leyland, G. H. John, R. T. Harley, M. M. Glazov, E. L. Ivchenko, D. A. Ritchie, I. Farrer, A. J. Shields, and M. Henini, Phys. Rev. B **75**, 165309 (2007).
  - <sup>57</sup> X. Z. Ruan, H. H. Luo, Y. Ji, Z. Y. Xu, and V. Umansky, Phys. Rev. B **77**, 193307 (2008).